



Toxicity assessment of reduced graphene oxide and titanium dioxide nanomaterials on gram-positive and gram-negative bacteria under normal laboratory lighting condition

N.S. Ahmad, N. Abdullah*, F.M. Yasin

Department of Chemical and Environmental Engineering, Faculty of Engineering, Universiti Putra Malaysia, UPM Serdang, Selangor, Malaysia



ARTICLE INFO

Keywords:

Bacillus subtilis
Escherichia coli
 Reduce graphene oxide
 Titanium dioxide
 Toxicity assessment

ABSTRACT

Toxicity effect of reduced graphene oxide (rGO) and titanium dioxide (TiO₂) nanomaterials (NMs) on Gram-positive (*Bacillus subtilis*) and Gram-negative (*Escherichia coli*) bacteria was assessed. For both strains, study demonstrated that the toxicity was time and concentration dependent which led to reduction in growth rate and cell death. Upon NMs exposure, an instantaneous cell death in *E. coli* culture was observed. This is in contrast with *B. subtilis*, in which the culture growth remained in the log phase; however their growth rate constant, μ_g was reduced by ~70%. The discrepancy between *E. coli* and *B. subtilis* was due to strain-specific response upon contact with NMs. TEM, SEM and EDX analysis revealed direct physical surface-surface interaction, as evidence from the adherence of NMs on the cell surface.

1. Introduction

Nanomaterials (NMs) are used for various purposes and functions in wide range of technologies such as drug delivery design of pharmaceuticals [1], biosensors [2], electronic devices [3], and photocatalysts [4], to name a few. Graphene family nanomaterials, such as graphene oxide (GO) and reduced graphene oxide (rGO), have recently been put under scientific attention for their potential in variety of applications, owing to their good thermal stability, high electronic conductivity, and excellent mechanical strength [5]. While, titanium dioxide (TiO₂) either in the fine (> 100 nm) or ultrafine (< 100 nm) particles are commercially used in fields of coatings and paints, wastewater treatment, and cosmetics due to its appropriate physicochemical properties for the intended functions [6]. For such frequent use of NMs (from the past, current and future), will increase the risk of its release to the environment. Public debate is emerging on issues pertaining the toxicological effect and environmental health from direct and indirect exposure of nanoparticles in commercial products [7]. Surprisingly, the access to the nano-toxicology data for most manufactured nanoparticles is limited even though this field is at fast growing phase.

Time of exposure, size, and concentration of nanoparticles are among factors contributing to the toxicity effect. When delivered in the same mass dose, smaller size materials showed higher toxicity as compared to the larger ones [8–12]. Nanoparticles forms of TiO₂ and CuO were found to be more toxic than their bulk forms particles against

microalgae *Pseudokirchneriella subcapitata* culture [8]. Similar observation was reported for other nanomaterials of ZnO, SiO₂, and Al₂O₃ in which their bulk forms exhibited lower toxicity compared to their particulate forms [10]. Smaller size of NMs not only exhibited higher surface area, but also have the ability to cross membrane barrier and accumulate within cells [13,14]. The accumulation of NMs within the bacterial membrane was reported to result in cells death [15].

Many researchers found a direct proportional relationship between cells death and exposure time [16–19], and between cells death and nanoparticle concentration [16,20]. The longer the cell culture exposed to nanoparticles, the higher the cell death reported [18,19]. This profile was observed in different studies on varieties of nanoparticles such as ZnO [18], GO [19], TiO₂ [21] and AgNO₃ [22]. The effect of NM concentration on cell viability was studied using graphene nanoplatelets [23], silver [24] and TiO₂ [25]. A significant cell death was observed when exposed to 1 µg/mL (low concentration) of rGO. By increasing the dose of rGO to 100 µg/mL, complete cell death was reported [23], indicating a direct toxicity relationship with NM dosage. In contrast, separate studies conducted by Takenaka et al. [24] and Gurr et al. [25] on silver and TiO₂ NMs, respectively, revealed that the lower concentration showed enhanced toxicity as compared to the higher concentration. Reason for this is due to the formation of NM aggregates in a culture containing higher NM concentration, leading to reduction in the overall toxicity [25].

Variety of nanomaterials such as TiO₂, Fe₂O₃, AgO and ZnO are

* Corresponding author.

E-mail address: nhafizah@upm.edu.my (N. Abdullah).

<https://doi.org/10.1016/j.toxrep.2020.04.015>

Received 12 November 2019; Received in revised form 27 April 2020; Accepted 30 April 2020

Available online 19 May 2020

2214-7500/© 2020 Published by Elsevier B.V. This is an open access article under the CC BY-NC-ND license

(<http://creativecommons.org/licenses/by-nc-nd/4.0/>).

widely used as antimicrobial coating in many products. These nanomaterials had great antimicrobial resistance towards microorganism [8,14,26–28]. Microbial cultures such as bacteria, yeast, fungi and algae are commonly used to assess the antimicrobial properties of a specific nanomaterial. Bacterial strains, either belong to Gram-negative and Gram-positive are known to cause major public health problems. They response differently when exposed to different nanomaterial. For instance, both Gram-positive and Gram-negative bacteria are sensitive to TiO₂ [29–31]. Nevertheless, Gram-negative *E. coli* was found to be less sensitive to TiO₂ than Gram-positive *B. subtilis* and *B. megaterium* [29,30,32]. Gram-negative bacteria have more complex cell wall structure with two (outer and inner) cell membranes. The outer membrane influences the permeability of molecules, acts as additional barrier and therefore a probable explanation for their higher resistant against chemical agents under certain condition compared to Gram-positive bacteria [29].

Contradict to the above findings, other studies reported that Gram-negative bacteria to be more sensitive as compared to Gram-positive bacteria against TiO₂ [31] GO [33], Ag [34], and CuO [35]. Pal et al. [31]. and Azam et al. [14] reported that Gram-negative *E. coli* has a negative surface charge which enhances the interaction with positive charge NMs. *E. coli* cells could attract lower charged cations per cell basis, as a result, higher cytotoxicity might be exerted at the lower valent cations [37]. The attachment of nanoparticles on microorganism may mechanically damage the cell wall causing the nanoparticles to penetrate into the cells, leaking of all cell constituents and eventually lead to cell death [38]. The other possible reason would be, Gram-negative bacteria possess a thin peptidoglycan layer with 7–8 nm thickness, while Gram-positive bacteria consists of thick peptidoglycan layer with 20–80 nm thickness [33]. Thicker peptidoglycan layer prevent the penetration of nanoparticles into the cytoplasm [22]. Besides, Gram-positive *B. subtilis* strain is known as spore-forming bacteria. Spore cell have much thicker and robust proteinous cell wall, and act as a major barrier for the nanoparticles from entering the cell [39]. The variation of sensitivity of Gram-negative and Gram-positive bacteria could be due to differences in physiology, metabolism, cell structures, or degree of contact of organism with nanoparticles [35]. Other than bacteria, variation in toxicity effect of NP was also reported in other culture, such as yeast [9], fungus [40], human cells [25], nematodes [41], and crustaceans [42].

Owing the intrinsic properties such as small size and high specific area, toxicity of rGO and TiO₂ must take into account as it is very useful in various applications. From our best knowledge, there is no other research done to compare the toxicity between carbon-based rGO and metal oxide TiO₂ NPs using both Gram-positive and Gram-negative. Their toxicity effect on bacterial cells of Gram-positive and Gram-negative under different exposure times and concentrations was studied. Culture of *B. subtilis* and *E. coli* was used to represent Gram-positive and Gram-negative, respectively. Cell viability and death were monitored and quantified using selective Trypan blue staining, under direct microscopic observation. The morphological assessment of the cell structure when exposed to NMs was conducted via scanning and transmission electron microscopy with EDX to trace the deposition pattern of NMs in the cell culture.

2. Materials and methods

2.1. Materials

B. subtilis subsp. *spizizenii* Nakamura et al. (ATCC® 6633™) was purchased from ATCC (USA). *E. coli* (ATCC® 25922™) was donated from culture collection at Faculty of Biotechnology and Biomolecular Sciences, UPM (Malaysia). Titanium dioxide (TiO₂) (13463-67-7) powders range of 50–500 nm (anatase and rutile) were purchased from Sigma-Aldrich (New Jersey) while reduced graphene oxide (rGO) (7782-42-5) was prepared in-house using chemical exfoliation

technique [43] with further modification [44]. Luria- Bertani (LB) medium, trypan blue and glycerol were also purchased from Sigma-Aldrich (New Jersey) and used directly without any further purification. All aqueous solutions were prepared with deionized water.

2.2. Characterization of NMs

For NMs imaging, NMs powder was mounted onto the stub and coated with gold. Then, the samples were analyzed with SEM and EDX (S-3400 N, Hitachi, Japan).

2.3. Preparation of NMs suspension

NM powder was suspended in deionized water until reach the final concentration of 50, 100, and 150 µg/mL. The solutions then were sonicated in water bath sonicator (Branson, model 1510, USA) at 40 kHz under 185 W for 30 min to avoid agglomeration of NMs.

2.4. Preparation of bacterial culture

B. subtilis and *E. coli* were grown overnight in LB medium at 37 °C and 180 rpm. The cultures were harvested at the exponential growth phase via centrifugation (LMC-3000, Biosan, Latvia) at 3000 rpm for 10 min. The cells were washed twice with deionized water to remove residual macromolecules and other growth medium constituents. Then the cell pellets were resuspended in LB medium. It was stored at –10 °C until use.

2.5. Quantification of cell viability using trypan blue staining method

B. subtilis and *E. coli* culture were grown in LB medium at 37 °C under 180 rpm shaking speed for 24 h. At the interval of 0, 6, and 24 h incubation time, viable and non viable cells were counted using hemocytometer cell counting. 100 µL of sample was gently mixed with 100 µL of 0.4 % trypan blue dye and left to stand for 5 min. 20 µL of cell suspension was loaded into each chamber of hemocytometer and analyzed under a 40 × magnification of light microscope (DM3000, Leica, Germany). Non viable cells stained blue, while viable cells appear unstained under a microscope. After 24 h growth incubation time, cell culture was added with a known amount of rGO and TiO₂ (anatase and rutile). Then cultures were left for further incubation until 96 h. The numbers of viable and non viable cells were counted at daily time interval. Numbers of cells were counted and compared with negative control (cell culture without NMs) (Fig. 1).

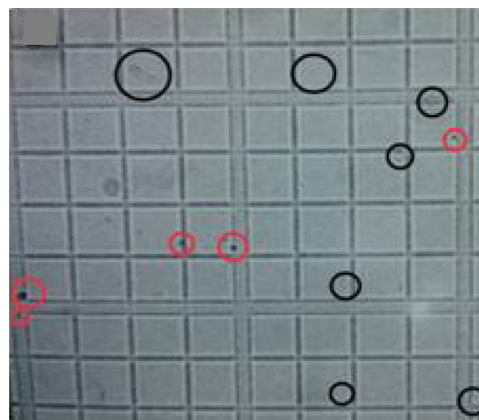


Fig. 1. Cells with trypan blue dye under light microscope. The black circle referring to viable cells, while red circle referring to nonviable cells. (For interpretation of the references to colour in this figure legend, the reader is referred to the web version of this article.)

2.6. Cell morphology observation

The cell cultures were harvested via centrifugation. The samples were fixed in 2.5 % glutaraldehyde for six hours at 4 °C. The samples were further centrifuged (MiniSpin, Eppendorf, Germany) to remove the liquid form and washed with 0.1 M of sodium cacodylate buffer for three times. It was stand for 10 min after each washing process. The samples were then post fix in 1% of osmium tetroxide for two hours at 4 °C and washed with 0.1 M of sodium cacodylate buffer for three times. It was stand for 10 min after each washing process. It was then put into critical dier (EM CPD030, Leica, Germany) for 30 min, mounted onto the stub, and coated with gold. The samples were analyzed with SEM (S-3400 N, Hitachi, Japan). For TEM analysis, the specimen was infiltrated with acetone and resin mixture, placed into beam capsule and filled up with resin. It was then polymerized in oven at 60 °C for 24 h. The specimen was cut, stained with uranyl acetate for 15 min, before observation under TEM (JEM-2100 F, Joel, USA).

2.7. Statistical analysis

At least three independent experiments were carried out in triplicates for each evaluation. All data were expressed as the mean and standard deviation.

3. Results and discussion

3.1. Characterization of rGO and TiO₂ NMs

SEM images of reduced graphene oxide revealed that it consists of non-particulate, thin, crumpled (Fig. 2a), folded (Fig. 2b), flower-like (Fig. 2c) and wrinkle shape at the edge. The folded regions of the rGO sheets were found to have the average width of < 100 nm by high resolution SEM. From SEM images (Fig. 3), small and sphere shape of rutile and anatase TiO₂ NPs were observed and their dimension varied in a narrow range of 70–130 nm for anatase, while rutile has the size about 90–200 nm. There was no apparent morphology structure different between both TiO₂ types. Although NPs aggregation was observed in this study, there were some particles still in individual nano sized particles in the solution. Sonication process was taken place to reduce the degree of agglomeration.

3.2. Effect of rGO and TiO₂ on bacterial growth

The effect of NMs on the growth of *B. subtilis* and *E. coli* culture was performed in LB medium dosed with 100 µg/mL NMs for 96 h, Fig. 4 and Fig. 5, respectively. In the absence of NMs (control), both *B. subtilis* and *E. coli* displayed similar growth profile consisted on log growth, stationary and death phase. Since all the cultures were used at their log phase, there was no lag phase observed. Exposure to NMs showed different outcomes between *B. subtilis* and *E. coli*. With respect to their control culture, deviations were observed in the length and onset time

of exponential, stationary and death phase (Table 1 and Table 2).

NMs caused a growth inhibition towards both microbes, but in different manner. Upon exposure to NMs, the viable cell count of *E. coli* dropped significantly as compared to the control culture (Fig. 5) This leads to an early onset of death phase at the 20th hour for anatase TiO₂ and the 40th hour for both rGO and rutile TiO₂, as with comparison to the 72nd hour for the onset of death phase in control culture. The death rate constant, k_D vary slightly among these NMs, ranging from 0.024–0.035 h⁻¹ with anatase TiO₂ gave the most toxic impact to the culture amounting to 75 % cell death at the end of the 96 h incubation time. Culture dosed with rGO resulted in 50 % reduction and this was in agreement with previous work by Li et al. [40], whom observed a reduction of viable cell by 46 % when exposed to 40 µg/mL rGO.

Different toxicity impact was observed in *B. subtilis* culture (Fig. 4) than that in *E. coli* culture (Fig. 5). Exposure to the NMs did cause some damaging to cells growth, however did not lead to sudden reduction in cell viability. Upon exposure to the NMs at the 24th hour of growth, cells were found to continuing their log growth phase however at slower growth rate with 70 % reduction in μ_g from 0.1 h⁻¹ to 0.03 h⁻¹ for both rGO and rutile TiO₂ culture. For anatase TiO₂, the cell entered stationary phase right after the its exposure and remained at that phase through the 96 h incubation period, with no apparent death phase. This may indicates that cells developed some degree tolerance against TiO₂ present in the environment.

The differential toxicity impact from NMs exposure of Gram-positive versus Gram-negative bacteria is probably due to the differences in their cell wall structure. Gram-positive bacteria possess a thick peptidoglycan layer (~20–80 nm) while Gram-negative bacteria have a thin peptidoglycan layer (7–8 nm) [33]. However, Gram-negative cell wall is composed of complex membrane with two cell membranes, a plasma membrane, and an outer membrane whereas, only plasma membrane appear in Gram-positive bacteria. The addition of the outer membrane in Gram-negative bacteria cells affects the permeability of molecules [29]. While this result is similar to the research conducted by Azam et al. [14] and Yoon et al. [45] on the antibacterial activities of other metal oxide nanomaterial, but it is in contradict with a studied by Azam et al. [35] and Rincon and Pulgarin [31]. Strain of *B. subtilis* is known to be a spore forming bacteria. Since the spore cells contain much thicker and robust proteinous cell wall, thus reduce the ability of nanoparticles to across the cell membrane [39]. In short, the resistance of microorganisms against nanoparticles is not only dependent on the type of bacteria, but also other factors, namely the mechanisms involved in the cytotoxicity of nanoparticles itself and others.

Anatase TiO₂ dispersion exhibited the highest antibacterial activity, sequentially followed by rGO and rutile TiO₂ (Fig. 4) on both *E. coli* and *B. subtilis* culture. Both NMs are known to be very damaging to cells, as evidenced in this present study. Specifically, the degree of inhibition of anatase TiO₂ was 2.7 and 2.2 fold greater than rutile TiO₂ and rGO, respectively after being exposed to *E. coli* culture. When comparing the toxicity of anatase and rutile forms of TiO₂ NPs, several factors can be considered. Based on the SEM image, anatase NPs (70–130 nm) was

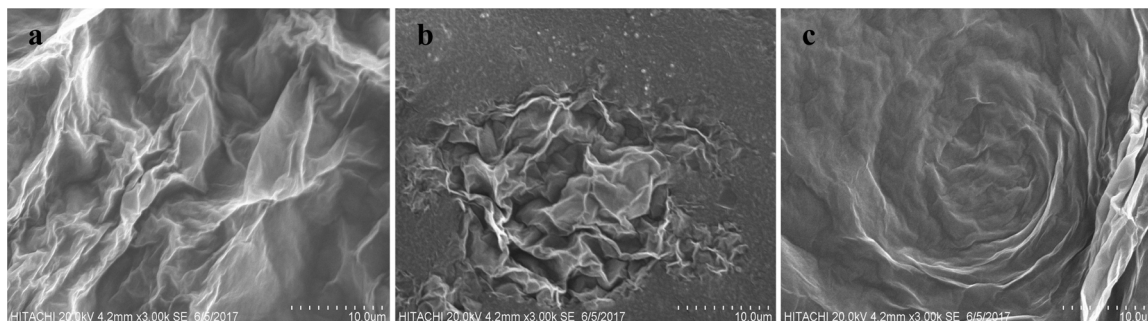


Fig. 2. SEM images rGO NPs consist of a) crumpled b) folded and c) flower-like shape.

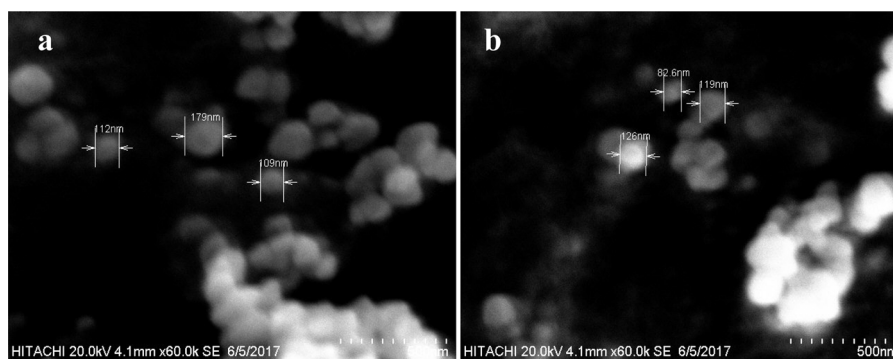


Fig. 3. SEM images of a) rutile and b) anatase TiO₂ nanoparticles.

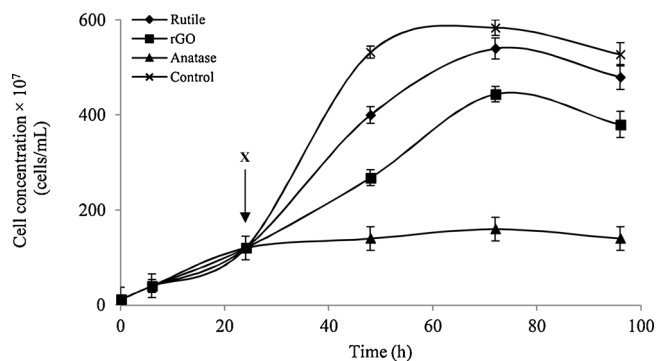


Fig. 4. Growth of *B. subtilis* treated with rGO and TiO₂ at 37 °C for 96 h and 180 rpm shaking speed. Growth inhibition were determined by Trypan blue staining using hemocytometer cell counting method and expressed as percentage of control. X defined as the time of NMs dosage. Error bars represent the standard error of the mean.

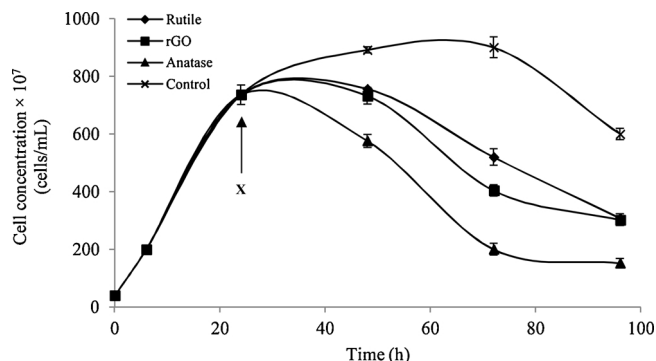


Fig. 5. Growth of *E. coli* treated with rGO and TiO₂ at 37 °C for 96 h and 180 rpm shaking speed. Growth inhibition were determined by Trypan blue staining using hemocytometer cell counting method and expressed as percentage of control. X defined as the time of NMs dosage. Error bars represent the standard error of the mean.

smaller compared to rutile (90–200 nm) particles. Smaller particles have higher surface area and particle number per unit mass. Result from the current study showed significant growth inhibition of rGO towards

all test models. One possible reason is due to the direct contact of sharp edge of rGO nanosheets with the cell wall that may cause the cell membrane damage. The toxicity of TiO₂ and rGO was reported mainly due to the generation of reactive oxygen species (ROS), even under normal laboratory lighting condition [46] and superoxide radical anion species. This was similar to previous study where 20 % growth reduction of *Staphylococcus aureus* (Gram positive bacteria) was recorded when exposed to TiO₂ under normal laboratory lighting condition [47]. Meanwhile, the interaction between graphene nanosheets and bacterial surface was claimed to lead to the cell death [33]. The mechanism of antimicrobial action applicable to graphene-based materials has been proposed by Liu et al. [17], consisted of propose three steps mechanism, i) deposition of cells on graphene-based materials, ii) membrane and oxidative stress caused by direct contact of sharp edge graphene-based materials, and iii) oxidation of superoxide anion.

3.3. Concentration-dependent antibacterial activity of rGO and TiO₂

The concentration dependence of antibacterial activities on rGO and TiO₂ NMs were determined at different concentrations (50, 100 and 150 µg/mL) for a duration of 24 h at 37 °C. In general, results showed a concentration-dependent on antibacterial activity with direct proportional relationship between them. Fig. 6 and Fig. 7 showed growth inhibition of *B. subtilis* and *E. coli* increases with the increase dose of rGO and TiO₂ concentration, respectively. Increasing the concentration of NM increases the growth inhibition, indicates that concentration of NMs itself is one of prime parameter for the antimicrobial activity.

Both rGO and TiO₂ exhibited significant toxicity effects even at low concentration of 50 µg/mL after 24 h of incubation time. Nevertheless, the maximum loss of *B. subtilis* and *E. coli* viabilities was recorded at 150 µg/mL concentration for both rGO and TiO₂ nanoparticles. Among of these nanoparticles, TiO₂ in anatase form was strongly inhibit the growth of *B. subtilis* and *E. coli* cultures at 150 µg/mL, with the growth inhibition of 76 % and 40 %, respectively. rGO was recorded to be the mild toxic nanoparticles, while rutile form was the least toxic in both bacterial samples. By increasing the nanoparticle concentration, it may raise the chance of interaction between cells and nanoparticles, thus increase in the loss of cell viability [48]. But, agglomeration of nanoparticles at higher concentration reduced the surface area [49] that may avoid direct interaction of it with bacteria, therefore reduce the cell wall penetration [10]. Graphene-based nanoparticles were reported to

Table 1
Growth phase and kinetics of *B. subtilis* culture with the present of respective NMs.

NMs	Lag phase (h)	Log phase (h)	Stationary phase (h)	Death phase (h)	μ_g (h ⁻¹)	$-k_d$ (h ⁻¹)	Final cell concentration (cell/mL)
Without NMs	–	24–56	56–72	72–96	0.0522	0.0042	528 ± 2.646
Anatase TiO ₂	–	24–72	–	72–96	0.0060	0.0056	140 ± 1.732
Rutile TiO ₂	–	24–72	–	72–96	0.0313	0.0049	480 ± 1.732
rGO	–	24–72	–	72–96	0.0273	0.0065	380 ± 2.000

Table 2
Growth phase and kinetics value of *E. coli* culture with the present of respective NMs.

NMs	Lag phase (h)	Log phase (h)	Stationary phase (h)	Death phase (h)	μ_g (h^{-1})	$-k_d$ (h^{-1})	Final cell concentration (cell/mL)
Without NMs	–	24–48	48–72	72–96	0.0080	0.0169	600 ± 3.606
Anatase TiO ₂	–	–	–	24–96	–	0.0241	152 ± 2.000
Rutile TiO ₂	–	–	24–40	40–96	–	0.0171	308 ± 1.000
rGO	–	–	24–40	40–96	–	0.0180	302 ± 2.64

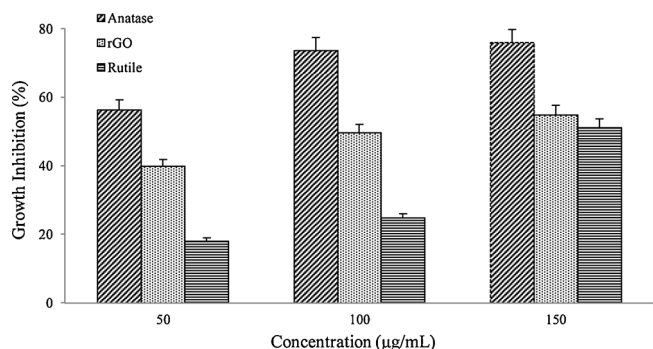


Fig. 6. Growth inhibition of *B. subtilis* treated with rGO and TiO₂ at 37 °C for 24 h and 180 rpm shaking speed. Growth inhibition were determined by Trypan blue staining using hemocytometer cell counting method and expressed as percentage of control. Error bars represent the standard error of the mean.

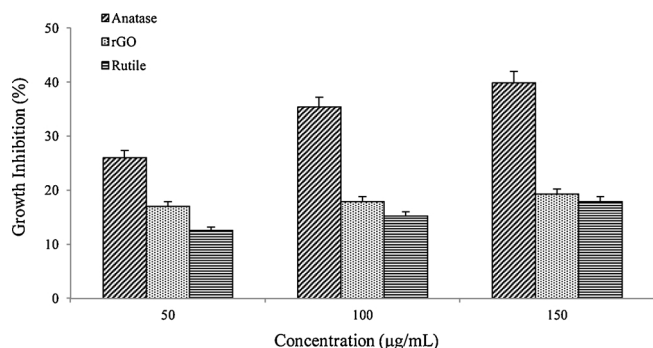


Fig. 7. Growth inhibition of *E. coli* treated with rGO and TiO₂ at 37 °C for 24 h and 180 rpm shaking speed. Growth inhibition were determined by Trypan blue staining using hemocytometer cell counting method and expressed as percentage of control. Error bars represent the standard error of the mean.

exhibit excellent antibacterial properties with mild cytotoxicity. A report by Hu et al. [37] stated that a reduction in the metabolic activity of *E. coli* as the concentration of GO and rGO increased from 20 to 85 µg/mL. A separate work by Tu et al. [50] reported that a possible mechanism of direct contact between the sharp edge of GO with *E. coli* causing induction of outer and inner cell membranes degradation, subsequently lead to cell death.

3.4. Time-dependent antibacterial activity of rGO and TiO₂

Time-dependent antibacterial activity of NPs was evaluated by dosing the culture with 50 µg/mL of NPs at the mid log phase of their growth and left to further incubate for 96 h. Fig. 8 and Fig. 9 showed the percentage of viable cell versus time for both *B. subtilis* and *E. coli* cultures, dosed with different NMs, respectively. In general, the present of NMs in their culture media causing viable cell to decrease in number. Prolonged incubation leads to further reduction in the cell viability in all cultures. At the end of the 96th hour, different percentage of viable cell remained in *B. subtilis* (ca. 30–50 %) as compared to *E. coli* (ca. 50–60 %). On other word, *E. coli* is more robust compared to *B. subtilis* when exposed with same NMs under same condition. This may be due

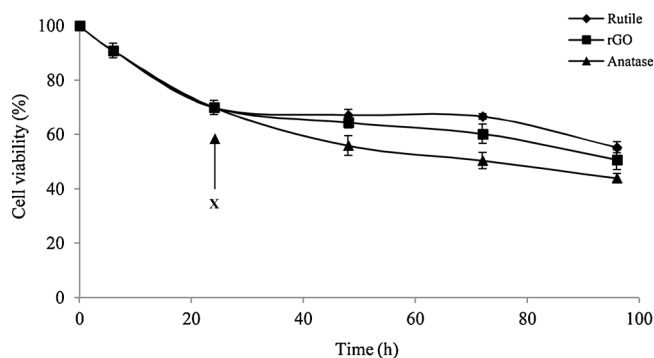


Fig. 8. Percentage of *B. subtilis* remained after treated with rGO and TiO₂ at 37 °C and 180 rpm shaking speed. Cell viability was determined by hemocytometer cell counting method and expressed as percentage of control. X defined as the time of NMs dosage. Error bars represent the standard error of the mean.

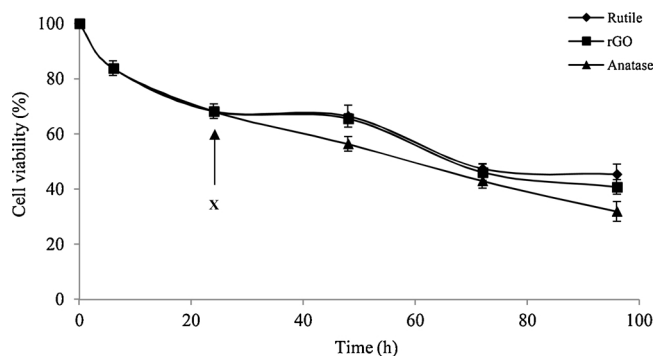


Fig. 9. Percentage of *E. coli* remained after treated with rGO and TiO₂ at 37 °C and 180 rpm shaking speed. Cell viability was determined by hemocytometer cell counting method and expressed as percentage of control. X defined as the time of NMs dosage. Error bars represent the standard error of the mean.

to differences in their cell membrane structure and composition, from which *B. subtilis* has a thinner peptidoglycan layer [33].

By increasing the incubation time, NPs had more chance to mingle around with the cells, attach to cell membrane, and therefore caused more membrane damage that lead to cell death. Similar trend also can be seen in the *E. coli* and *B. subtilis* cultures when incubated with NPs. This result was similar with other researcher [16,17], whom suggested that the antibacterial activity of NPs was time-dependent, and other researcher [18] found that none of *E. coli* and *B. subtilis* colony were detected for a longer NPs exposure as compared to a shorter exposure. Rincon and Pulgarin [27] reported that longer exposure time is required for bacterial inactivation if the initial concentration of bacteria is higher.

3.5. Morphological assessment of cell morphology when exposed to NMs and postulation of NMs deposition mechanism

SEM and TEM analysis were used to illustrate the interaction between nanoparticles and bacterial cultures. Cell exposed to NMs were observed under SEM imaging. Fig. 10a showed surface morphology of

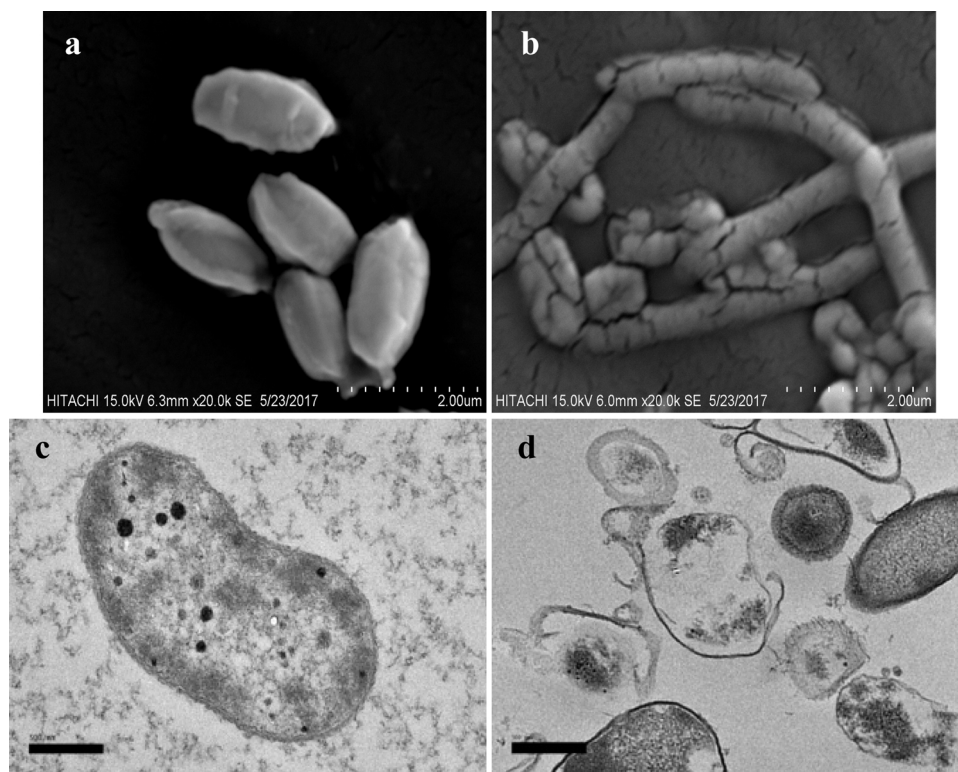


Fig. 10. Electron micrographs for a) surface scanning image of typical *B. subtilis* cell, b) surface scanning image of *B. subtilis* after exposure with anatase TiO₂, c) transmission cross-sectional image of *B. subtilis* cell and d) transmission cross-sectional image of *B. subtilis* after exposure with anatase TiO₂ NM.

B. subtilis cell having a short rod shaped with smooth surface structure. Upon exposure to TiO₂ (Fig. 10b), surface structure appeared to be severely damaged with appearance of fractures and cracks, lead to disintegration to cell integrity. The TEM image showing the internal cross section of cell structure (Fig. 10c) and upon exposure of TiO₂, the cell disintegration was observed in Fig. 10d and eventually caused cell to leak the cytoplasmic content to external. The similar phenomenon was observed for *E. coli*. [39], in which nanoparticles have penetrated inside the cell, causing the membrane damaged, however we did not observed this in our TEM analysis. After washed three times with deionized water, we found that titanium in both forms were still attach to the cell surface. This results proven that physical adherence of TiO₂ onto the cell surface, did take place when they are present in their growing culture media. The adherence mechanism may be due to physical adsorption via opposite charge. Stoimenov et al. [39] stated that the opposite charge of nanoparticles and bacteria may cause tighter binding between them, due to electrostatic forces. The roughness of TiO₂ nanoparticles also can increase the contact point between nanoparticles and cells causing damage at multiple points, which might eventually kill the microorganism [32]. The mechanism in which the NPs are able to cause the cell membrane damage and lead to cell death is not fully understood, but our study suggest that when cells were treated with NMs, changes were took place in its membrane that produced a major increase in its permeability affecting the proper transport through plasma membrane, causing the cells incapable of regulating transport properly through plasma membrane. In our study, it was believed that during direct contact between NMs and bacterial cells caused in the DNA damage and cellular protein become inactive.

4. Conclusion

Nanomaterials of rGO and TiO₂ (anatase and rutile) exhibited toxicity impact towards both *B. subtilis* and *E. coli*. In general, anatase TiO₂ is more toxic compared to rGO and rutile TiO₂. NMs caused

reduction in growth rate for *B. subtilis* with significant reduction in growth rate constant. In contrast, observation on the toxicity impact was slightly different in *E. coli*, where upon NMs exposure, the early onset of death phase was observed. The loss of viable cell by NMs exposure was found to be concentration and time dependent. Morphological observation had shown the adhesion of NMs on the cell surface and leading to disruption of cell membrane structure.

Declaration of competing interest

The authors declare that they have no known competing financial interests or personal relationships that could have appeared to influence the work reported in this paper.

Acknowledgements

The work is supported by PUTRA Grant (GP-1/2014/9443200), Universiti Putra Malaysia. Ms. Nurul Shahidah was financially funded by Graduate Research Fellowship, Universiti Putra Malaysia for the financial support of this research work.

References

- [1] H. Shen, L. Zhang, M. Liu, Z. Zhang, Biomedical applications of graphene, *Theranostics* 2 (2012) 283–294.
- [2] Y. Song, Y. Chen, L. Feng, J. Ren, X. Qu, Selective and quantitative cancer cell detection using target-directed functionalized graphene and its synergetic peroxidase-like activity, *Chem. Commun.* 47 (2011) 4436–4438.
- [3] Y. Liu, D. Yu, C. Zeng, Z. Miao, L. Dai, Biocompatible graphene oxide-based glucose biosensors, *Langmuir* 26 (2010) 6158–6160.
- [4] J.M. Macak, M. Zlamal, J. Krysa, P. Schmuki, Self-organized TiO₂ nanotube layers as highly efficient photocatalysts, *Small* 3 (2007) 300–304.
- [5] L. Horváth, A. Magrez, M. Burghard, K. Kern, L. Forró, B. Schwaller, Evaluation of the toxicity of graphene derivatives on cells of the lung luminal surface, *Carbon NY* 64 (2013) 45–60.
- [6] L. Ma, J. Liu, N. Li, J. Wang, Y. Duan, J. Yan, H. Liu, H. Wang, F. Hong, Oxidative stress in the brain of mice caused by translocated nanoparticulate TiO₂ delivered to the abdominal cavity, *Biomaterials* 31 (2010) 99–105.

- [7] R. Brayner, R. Ferrari-Iliou, N. Brivois, S. Djediat, M.F. Benedetti, F. Fiévet, Toxicological impact studies based on *Escherichia coli* bacteria in ultrafine ZnO nanoparticles colloidal medium, *Nano Lett.* 6 (2006) 866–870.
- [8] V. Aruoja, H.-C. Dubourguier, K. Kasemets, A. Kahru, Toxicity of nanoparticles of CuO, ZnO and TiO₂ to microalgae *Pseudokirchneriella subcapitata*, *Sci. Total Environ.* 407 (2009) 1461–1468.
- [9] K. Kasemets, A. Ivask, H.C. Dubourguier, A. Kahru, Toxicity of nanoparticles of ZnO, CuO and TiO₂ to yeast *Saccharomyces cerevisiae*, *Toxicol. Vitro.* 23 (2009) 1116–1122.
- [10] W. Jiang, H. Mashayekhi, B. Xing, Bacterial toxicity comparison between nano- and micro-scaled oxide particles, *Environ. Pollut.* 157 (2009) 1619–1625.
- [11] N. Hashizume, Y. Oshima, M. Nakai, T. Kobayashi, T. Sasaki, K. Kawaguchi, K. Honda, M. Gamoto, K. Yamamoto, Y. Tsubokura, S. Ajimi, Y. Inoue, N. Imatanaka, Categorization of nano-structured titanium dioxide according to physicochemical characteristics and pulmonary toxicity, *Toxicol. Reports* 3 (2016) 490–500.
- [12] S. Jahan, I. Yusoff, Y. Alias, A.F.A. Bakar, Reviews of the toxicity behavior of five potential engineered nanomaterials (ENMs) into the aquatic ecosystem, *Toxicol. Reports* 4 (2017) 211–220.
- [13] D. Xiong, T. Fang, L. Yu, X. Sima, W. Zhu, Effects of nano-scale TiO₂, ZnO and their bulk counterparts on zebrafish: acute toxicity, oxidative stress and oxidative damage, *Sci. Total Environ.* 409 (2011) 1444–1452.
- [14] A. Azam, A.S. Ahmed, M. Oves, M.S. Khan, S.S. Habib, A. Memic, Antimicrobial activity of metal oxide nanoparticles against Gram-positive and Gram-negative bacteria: a comparative study, *Int. J. Nanomedicine* 7 (2012) 6003–6009.
- [15] I. Sondi, B. Salopek-Sondi, Silver nanoparticles as antimicrobial agent: a case study on *E. coli* as a model for Gram-negative bacteria, *J. Colloid Interface Sci.* 275 (2004) 177–182.
- [16] S. Gurunathan, J.W. Han, A.A. Dayem, V. Eppakayala, J.H. Kim, Oxidative stress-mediated antibacterial activity of graphene oxide and reduced graphene oxide in *Pseudomonas aeruginosa*, *Int. J. Nanomedicine* 7 (2012) 5901–5914.
- [17] S. Liu, T.H. Zeng, M. Hofmann, E. Burcombe, J. Wei, R. Jiang, J. Kong, Y. Chen, Antibacterial activity of graphite, graphite oxide, graphene oxide, and reduced graphene oxide: membrane and oxidative stress, *ACS Nano* 5 (2011) 6971–6980.
- [18] K.R. Raghupathi, R.T. Koodali, A.C. Manna, Size-dependent bacterial growth inhibition and mechanism of antibacterial activity of zinc oxide nanoparticles, *Langmuir* 27 (2011) 4020–4028.
- [19] O. Akhavan, E. Ghaderi, *Escherichia coli* bacteria reduce graphene oxide to bactericidal graphene in a self-limiting manner, *Carbon* NY (2012).
- [20] S. Gurunathan, J.W. Han, A.A. Dayem, V. Eppakayala, M.R. Park, D.N. Kwon, J.H. Kim, Antibacterial activity of dithiothreitol reduced graphene oxide, *J. Ind. Eng. Chem.* 19 (2013) 1280–1288.
- [21] J.C. Ireland, P. Klostermann, E.W. Rice, R.M. Clark, Inactivation of *Escherichia coli* by titanium dioxide photocatalytic oxidation, *Appl. Environ. Microbiol.* 59 (1993) 1668–1670.
- [22] Q.L. Feng, G. Chen, J. Wu, G.Q. Chen, F.Z. Cui, T.N. Kim, J.O. Kim, A mechanistic study of the antibacterial effect of silver ions on *Escherichia coli* and *Staphylococcus aureus*, *J. Biomed. Mater. Res.* 52 (2000) 662–668.
- [23] O. Akhavan, E. Ghaderi, A. Akhavan, Size-dependent genotoxicity of graphene nanoplatelets in human stem cells, *Biomaterials* 33 (2012) 8017–8025.
- [24] S. Takenaka, E. Karg, C. Roth, H. Schulz, A. Ziesenis, U. Heinzmann, P. Schramel, J. Heyder, Pulmonary and systemic distribution of inhaled ultrafine silver particles in rats, *Environ. Health Perspect.* 109 (2001) 547–551.
- [25] J.R. Gurr, A.S.S. Wang, C.H. Chen, K.Y. Jan, Ultrafine titanium dioxide particles in the absence of photoactivation can induce oxidative damage to human bronchial epithelial cells, *Toxicology* 213 (2005) 66–73.
- [26] S. Nair, A. Sasidharan, V.V. Divya Rani, D. Menon, S. Nair, K. Manzoor, S. Raina, Role of size scale of ZnO nanoparticles and microparticles on toxicity toward bacteria and osteoblast cancer cells, *J. Mater. Sci. Mater. Med.* 20 (2009) 235–241.
- [27] A.G. Rincón, C. Pulgarin, Bactericidal action of illuminated TiO₂ on pure *Escherichia coli* and natural bacterial consortia: post-irradiation events in the dark and assessment of the effective disinfection time, *Appl. Catal. B Environ.* 49 (2004) 99–112.
- [28] M.R. Das, R.K. Sarma, R. Saikia, V.S. Kale, M.V. Shelke, P. Sengupta, Synthesis of silver nanoparticles in an aqueous suspension of graphene oxide sheets and its antimicrobial activity, *Colloids Surf. B Biointerfaces* 83 (2011) 16–22.
- [29] G. Fu, P.S. Vary, C.-T. Lin, Anatase TiO₂ nanocomposites for antimicrobial coatings, *J. Phys. Chem. B* 109 (2005) 8889–8898.
- [30] L.K. Adams, D.Y. Lyon, P.J.J. Alvarez, Comparative eco-toxicity of nanoscale TiO₂, SiO₂, and ZnO water suspensions, *Water Res.* 40 (2006) 3527–3532.
- [31] A.G. Rincón, C. Pulgarin, Use of coaxial photocatalytic reactor (CAPHORE) in the TiO₂ photo-assisted treatment of mixed *E. Coli* and *Bacillus* sp. And bacterial community present in wastewater, *Catal. Today* (2005) 331–344.
- [32] K.L. Yeung, W.K. Leung, N. Yao, S. Cao, Reactivity and antimicrobial properties of nanostructured titanium dioxide, *Catal. Today* 143 (2009) 218–224.
- [33] K. Krishnamoorthy, M. Veerapandian, L.H. Zhang, K. Yun, S.J. Kim, Antibacterial efficiency of graphene nanosheets against pathogenic bacteria via lipid peroxidation, *J. Phys. Chem. C* 116 (2012) 17280–17287.
- [34] J.S. Kim, E. Kuk, K.N. Yu, J.H. Kim, S.J. Park, H.J. Lee, S.H. Kim, Y.K. Park, Y.H. Park, C.Y. Hwang, Y.K. Kim, Y.S. Lee, D.H. Jeong, M.H. Cho, Antimicrobial effects of silver nanoparticles, *Nanomedicine Nanotechnol. Biol. Med.* 3 (2007) 95–101.
- [35] A. Azam, A.S. Ahmed, M. Oves, M.S. Khan, A. Memic, Size-dependent antimicrobial properties of CuO nanoparticles against Gram-positive and -negative bacterial strains, *Int. J. Nanomedicine* 7 (2012) 3527–3535.
- [37] X. Hu, S. Cook, P. Wang, H. Min Hwang, in vitro evaluation of cytotoxicity of engineered metal oxide nanoparticles, *Sci. Total Environ.* 407 (2009) 3070–3072.
- [38] B. Balusamy, Y.G. Kandhasamy, A. Senthambizhan, G. Chandrasekaran, M.S. Subramanian, T.S. Kumaravel, Characterization and bacterial toxicity of lanthanum oxide bulk and nanoparticles, *J. Rare Earths* 30 (2012) 1298–1302.
- [39] P.K. Stoimenov, R.L. Klinger, G.L. Marchin, K.J. Klabunde, Metal oxide nanoparticles as bactericidal agents, *Langmuir* 18 (2002) 6679–6686.
- [40] C. Li, X. Wang, F. Chen, C. Zhang, X. Zhi, K. Wang, D. Cui, The antifungal activity of graphene oxide-silver nanocomposites, *Biomaterials* 34 (2013) 3882–3890.
- [41] H. Wang, R.L. Wick, B. Xing, Toxicity of nanoparticulate and bulk ZnO, Al₂O₃ and TiO₂ to the nematode *Caenorhabditis elegans*, *Environ. Pollut.* 157 (2009) 1171–1177.
- [42] M. Heinala, A. Ivask, I. Blinova, H.C. Dubourguier, A. Kahru, Toxicity of nanosized and bulk ZnO, CuO and TiO₂ to bacteria *Vibrio fischeri* and crustaceans *Daphnia magna* and *Thamnocephalus platyurus*, *Chemosphere* 71 (2008) 1308–1316.
- [43] D. Li, S. Gilje, R.B. Kaner, G.G. Wallace, M.B. Mu, M.B. Muller, S. Gilje, R.B. Kaner, G.G. Wallace, Processable aqueous dispersions of graphene nanosheets, *Nat. Nanotechnol.* 3 (2008) 101–105.
- [44] N.I. Kovtyukhova, P.J. Ollivier, B.R. Martin, T.E. Mallouk, S.A. Chizhik, E.V. Buzaneva, A.D. Gorchinskiy, Layer-by-layer assembly of ultrathin composite films from micron-sized graphite oxide sheets and polycations, *Chem. Mater.* 11 (1999) 771–778.
- [45] K.-Y. Yoon, J. Hoon Byeon, J.-H. Park, J. Hwang, Susceptibility Constants of *Escherichia coli* and *Bacillus subtilis* to Silver and Copper Nanoparticles, (2007).
- [46] A. Simon-Deckers, S. Loo, M. Mayne-L'Hermite, N. Herlin-Boime, N. Menguy, C. Reynaud, B. Gouget, M. Carriere, Size-, composition- and shape-dependent toxicological impact of metal oxide nanoparticles and carbon nanotubes toward bacteria, *Environ. Sci. Technol.* 43 (2009) 8423–8429.
- [47] N. Jones, B. Ray, K.T. Ranjit, A.C. Manna, Antibacterial activity of ZnO nanoparticle suspensions on a broad spectrum of microorganisms, *FEMS Microbiol. Lett.* 279 (2008) 71–76.
- [48] S. Liu, M. Hu, T.H. Zeng, R. Wu, R. Jiang, J. Wei, L. Wang, J. Kong, Y. Chen, Lateral dimension-dependent antibacterial activity of graphene oxide sheets, *Langmuir* 28 (2012) 12364–12372.
- [49] Y. Zhou, Y. Kong, S. Kundu, J.D. Cirillo, H. Liang, Antibacterial activities of gold and silver nanoparticles against *Escherichia coli* and *Bacillus Calmette-Guérin*, *J. Nanobiotechnol.* 10 (2012) 19–27.
- [50] Y.S. Tu, M. Lv, P. Xiu, T. Huynh, M. Zhang, M. Castelli, Z.R. Liu, Q. Huang, C.H. Fan, H.P. Fang, R.H. Zhou, Destructive extraction of phospholipids from *Escherichia coli* membranes by graphene nanosheets, *Nat. Nanotechnol.* 8 (2013) 594–601.